

Mesoscopic Fluctuations of the Loschmidt Echo

Cyril Petitjean and Philippe Jacquod

Département de Physique Théorique, Université de Genève, CH-1211 Genève 4, Switzerland

(Dated: October 13 2004)

We investigate the time-dependent variance of the fidelity with which an initial narrow wavepacket is reconstructed after its dynamics is time-reversed with a perturbed Hamiltonian. In the semiclassical regime of perturbation, we show that the variance first rises algebraically up to a critical time t_c , after which it decays. To leading order in the effective Planck's constant \hbar_{eff} , this decay is given by the sum of a classical term $\simeq \exp[-2\lambda t]$, a quantum term $\simeq 2\hbar_{\text{eff}} \exp[-\Gamma t]$ and a mixed term $\simeq 2\exp[-(\Gamma + \lambda)t]$. Compared to the behavior of the average fidelity, this allows for the extraction of the classical Lyapunov exponent λ in a larger parameter range. Our results are confirmed by numerical simulations.

PACS numbers: 74.40.+k, 05.45.Mt, 03.65.Yz

Fluctuations of a physical quantity often contain more information than its average. For example, quantum signatures of classical chaos are absent of the average density of states, but strongly affect spectral fluctuations [1]. In the search for such signatures, another approach has been to investigate the sensitivity to an external perturbation that is exhibited by the quantum dynamics [2]. Going back to Ref. [3], the central quantity in this approach is the Loschmidt Echo [4], the fidelity

$$M(t) = |\langle \psi_0 | \exp[iHt] \exp[-iH_0t] | \psi_0 \rangle|^2 \quad (1)$$

with which an initial quantum state ψ_0 is reconstructed after the dynamics is time-reversed using a perturbed Hamiltonian, $H = H_0 + \epsilon V$ (we set $\hbar \equiv 1$). This approach proved very fruitful, however, most investigations of $M(t)$ (which we will briefly summarize below) considered the properties of the *average* fidelity $\overline{M(t)}$, either over different ψ_0 , or different elements of an ensemble of unperturbed Hamiltonians H_0 (having for instance the same classical Lyapunov exponent λ) and/or perturbation V . Curiously enough, the variance $\sigma^2(M)$ of the fidelity has been largely neglected so far. The purpose of this article is to fill this gap. We will see that the variance $\sigma^2(M)$ has a much richer behavior than $\overline{M(t)}$, allowing for the extraction of λ in a larger parameter range, and exhibiting a nonmonotonous behavior with a non-self-averaging maximal value $\sigma(t_c)/\overline{M(t_c)} \simeq 1$.

We first summarize what is known about the average fidelity $\overline{M(t)}$ in quantum chaotic systems. Three regimes of perturbation strength are differentiated by three energy scales [5]: the energy bandwidth B of H_0 , the golden rule spreading $\Gamma = 2\pi\epsilon^2 \overline{|\langle \phi_\alpha^{(0)} | V | \phi_\beta^{(0)} \rangle|^2} / \Delta$ of an eigenstate $\phi_\alpha^{(0)}$ of H_0 over the eigenbasis $\{\phi_\alpha\}$ of H , and the level spacing $\Delta = B\hbar_{\text{eff}}$ ($\hbar_{\text{eff}} = \nu^d/\Omega$ is the effective Planck's constant, given by the ratio of the wavelength volume to the system's volume). These three regimes are (i) the weak perturbation regime $\Gamma < \Delta$, with a typical Gaussian decay $\overline{M(t)} \simeq \exp(-\overline{\Sigma^2}t^2)$, $\Sigma^2 \equiv \epsilon^2(\langle \psi_0 | V^2 | \psi_0 \rangle - \langle \psi_0 | V | \psi_0 \rangle^2)$, $\overline{\Sigma^2} \simeq \Gamma\Delta\hbar_{\text{eff}}^{-1}$ [3, 6] (corrections to this Gaussian decay have been discussed in Ref. [7]), (ii) the semiclassical golden rule regime

$\Delta < \Gamma < B$, where the decay is exponential with a rate set by the smallest of Γ and λ , $\overline{M(t)} \simeq \exp[-\min(\Gamma, \lambda)t]$ [4, 5, 8], and (iii) the strong perturbation regime $\Gamma > B$ with another Gaussian decay $\overline{M(t)} \simeq \exp(-B^2t^2)$ [5]. This classification is based on the scheme of Ref. [5] which relates the behavior of $\overline{M(t)}$ to the local spectral density of eigenstates of H_0 over the eigenbasis of H [5, 9]. Accordingly, regime (ii) corresponds to the range of validity of Fermi's golden rule, where the local spectral density has a Lorentzian shape [5, 9, 10]. Quantum disordered systems with diffractive impurities, on the other hand, have been predicted to exhibit golden rule decay $\propto \exp[-\Gamma t]$ and Lyapunov decay $\propto \exp[-\lambda t]$ in different time intervals for a single set of parameters [12]. It is also worth mentioning that regular systems exhibit a very different behavior, where in the semiclassical regime (ii), $\overline{M(t)}$ decays as a power-law [13] (see also Ref. [14]). Finally, while in chaotic systems the averaging procedure has been found to be ergodic, i.e. considering different states ψ_0 is equivalent to considering different realizations of H_0 or V , the Lyapunov decay exists only for specific choices where ψ_0 has a well defined classical meaning, like a coherent or a position state [4, 11, 15, 16].

Investigations beyond this qualitative picture have focused on crossover regions between the regimes (i) and (ii) [7] and deviations from the behavior (ii) $\simeq \exp[-\min(\Gamma, \lambda)t]$ due to action correlations in weakly chaotic systems [17]. Ref. [18] provides the only analytical investigation of fluctuations of $M(t)$ to date. It shows that, for classically large perturbations, $\Gamma \gg B$, $\overline{M(t)}$ is dominated by very few exceptional events, so that a typical ψ_0 's fidelity is better described by $\exp[\ln(\overline{M})]$, and that $M(t)$ does not fluctuate after the Ehrenfest time $t_E = \lambda^{-1} |\ln[\hbar_{\text{eff}}]|$. We will see that these conclusions do not apply to the regime (ii) of present interest. While some numerical data for the distribution of $M(t)$ in the weak perturbation regime (i) were presented in Ref. [19], we focus here on chaotic systems and investigate the behavior of $\sigma^2(M)$ in the semiclassical regime (ii).

We first follow a semiclassical approach along the lines of Ref. [4]. We consider an initial Gaussian wavepacket $\psi_0(\mathbf{r}'_0) = (\pi\nu^2)^{-d/4} \exp[i\mathbf{p}_0 \cdot (\mathbf{r}'_0 - \mathbf{r}_0) - |\mathbf{r}'_0 - \mathbf{r}_0|^2/2\nu^2]$,

and approximate its time-evolution by

$$\langle \mathbf{r} | \exp(-iH_0 t) | \psi_0 \rangle = \int d\mathbf{r}'_0 \sum_s K_s^{H_0}(\mathbf{r}, \mathbf{r}'_0; t) \psi_0(\mathbf{r}'_0),$$

$$K_s^{H_0}(\mathbf{r}, \mathbf{r}'_0; t) = \frac{C_s^{1/2}}{(2\pi i)^{d/2}} \exp[iS_s^{H_0}(\mathbf{r}, \mathbf{r}'_0; t) - i\pi\mu_s/2].$$

The semiclassical propagator is expressed as a sum over classical trajectories (labelled s) connecting \mathbf{r} and \mathbf{r}'_0 in the time t . For each s , the partial propagator contains the action integral $S_s^H(\mathbf{r}, \mathbf{r}'_0; t)$ along s , a Maslov index μ_s , and the determinant C_s of the stability matrix [21]. We recall that this approach allows to calculate the time evolution of smooth, localized wavepackets up to algebraically long times $\propto \mathcal{O}(\hbar_{\text{eff}}^{-a}) \gg t_E$ (with $a > 0$) [22].

The fidelity then reads,

$$M(t) = \left| \int d\mathbf{r}_1 \int d\mathbf{r}'_0 \int d\mathbf{r}''_0 \psi_0(\mathbf{r}'_0) \psi_0^*(\mathbf{r}''_0) \right. \\ \left. \times \sum_{s_1, s_2} K_{s_1}^{H_0}(\mathbf{r}_1, \mathbf{r}'_0; t) [K_{s_2}^H(\mathbf{r}_1, \mathbf{r}''_0; t)]^* \right|^2 \quad (3)$$

We want to calculate $M^2(t)$. Squaring Eq. (3), we see that $M^2(t)$ is given by eight sums over classical paths and twelve spatial integrations. Noting that ψ_0 is a narrow Gaussian wavepacket, we first linearize all eight action integrals around \mathbf{r}_0 ,

$$S_s(\mathbf{r}, \mathbf{r}'_0; t) \simeq S_s(\mathbf{r}, \mathbf{r}_0; t) - (\mathbf{r}'_0 - \mathbf{r}_0) \cdot \mathbf{p}_s. \quad (4)$$

We can then perform the Gaussian integrations over the eight initial positions \mathbf{r}'_0 , \mathbf{r}''_0 and so forth. In this way $M^2(t)$ is expressed as a sum over eight trajectories connecting \mathbf{r}_0 to four independent final points \mathbf{r}_j over which one integrates,

$$M^2(t) = \int \prod_{j=1}^4 d\mathbf{r}_j \sum_{s_i; i=1}^8 \exp[i(\Phi^{H_0} - \Phi^H - \pi\mathcal{M}/2)] \\ \times \left(\prod_i C_{s_i}^{1/2} \left(\frac{\nu^2}{\pi} \right)^{d/4} \exp(-\nu^2 \delta \mathbf{p}_{s_i}^2 / 2) \right), \quad (5)$$

where we introduced $\mathcal{M} = \sum_{i=0}^3 (-1)^i (\mu_{s_{2i+1}} - \mu_{s_{2i+2}})$ and $\delta \mathbf{p}_{s_i} = \mathbf{p}_{s_i} - \mathbf{p}_0$.

The expression of Eq. (5) is schematically described in Fig. 1. Classical trajectories are represented by a full line if they correspond to H_0 and a dashed line for H , with an arrow indicating the direction of propagation. In the semiclassical limit $S_s \gg 1$ (we recall that actions are expressed in units of \hbar), Eq. (5) is dominated by terms which satisfy a stationary phase condition, i.e. where the variation of the difference of the two action phases

$$\Phi^{H_0} = S_{s_1}^{H_0}(\mathbf{r}_1, \mathbf{r}_0; t) - S_{s_3}^{H_0}(\mathbf{r}_0, \mathbf{r}_2; t) \\ + S_{s_5}^{H_0}(\mathbf{r}_4, \mathbf{r}_0; t) - S_{s_7}^{H_0}(\mathbf{r}_0, \mathbf{r}_3; t), \quad (6a)$$

$$\Phi^H = S_{s_2}^H(\mathbf{r}_0, \mathbf{r}_1; t) - S_{s_4}^H(\mathbf{r}_2, \mathbf{r}_0; t) \\ + S_{s_6}^H(\mathbf{r}_0, \mathbf{r}_4; t) - S_{s_8}^H(\mathbf{r}_3, \mathbf{r}_0; t), \quad (6b)$$

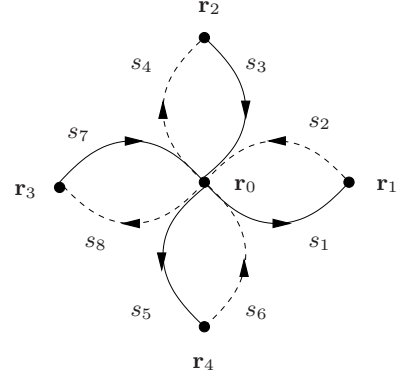


Figure 1: Diagrammatic representation of the squared fidelity $M^2(t)$.

has to be minimized. These stationary phase terms are easily identified from the diagrammatic representation as those where two classical trajectories s and s' of opposite direction of propagation are *contracted*, i.e. $s = s'$, up to a quantum resolution given by the wavelength ν [23]. This is represented in Fig. 2 by bringing two lines together in parallel. Contracting either two dashed or two full lines allows for an almost exact cancellation of the actions, hence an almost perturbation-independent contribution, up to a contribution arising from the finite resolution ν with which the two paths overlap. However when a full line is contracted with a dashed line, the resulting contribution still depends on the action $\delta S_s = -\epsilon \int_s V(\mathbf{q}(t), t)$ accumulated by the perturbation along the classical path s , spatially parametrized as $\mathbf{q}(t)$. Since we are interested in the variance $\sigma^2(M) = \overline{M^2} - \overline{M}^2$ (this is indicated by brackets in Fig. 2) we must subtract the terms contained in $\overline{M^2}$ corresponding to independent contractions in each of the two subsets (s_1, s_2, s_3, s_4) and (s_5, s_6, s_7, s_8) . Consequently, all contributions to $\sigma^2(M)$ require pairing of spatial coordinates, $|\mathbf{r}_i - \mathbf{r}_j| \leq \nu$, for at least one pair of indices $i, j = 1, 2, 3, 4$.

With these considerations, the four dominant contributions to $\sigma^2(M)$ are depicted on the right-hand side of Fig. 2. The first one corresponds to $s_1 = s_2 \simeq s_7 = s_8$ and $s_3 = s_4 \simeq s_5 = s_6$, which requires $\mathbf{r}_1 \simeq \mathbf{r}_3$, $\mathbf{r}_2 \simeq \mathbf{r}_4$. This gives a contribution

$$\sigma_1^2 = \left(\frac{\nu^2}{\pi} \right)^{2d} \left\langle \int d\mathbf{r}_1 d\mathbf{r}_3 \sum C_{s_1}^2 \right. \\ \left. \times \exp[-2\nu^2 \delta \mathbf{p}_{s_1}^2 + i\delta \Phi_{s_1}] \Theta(\nu - |\mathbf{r}_1 - \mathbf{r}_3|) \right\rangle^2, \quad (7)$$

where $\delta \Phi_{s_1} = \epsilon \int_0^t dt' \nabla V[\mathbf{q}(t')] [\mathbf{q}_{s_1}(t') - \mathbf{q}_{s_7}(t')]$ arises from the linearization of V on $s = s_{1,2} \simeq s' = s_{7,8}$ [4, 11], and $\mathbf{q}_{s_1}(\hat{t})$ lies on s_1 with $\mathbf{q}(0) = \mathbf{r}_0$ and $\mathbf{q}(t) = \mathbf{r}_1$. In Eq. (7) the integrations are restricted by $|\mathbf{r}_1 - \mathbf{r}_3| \leq \nu$ because of the finite resolution with which two paths can be equated (this is also enforced by the presence

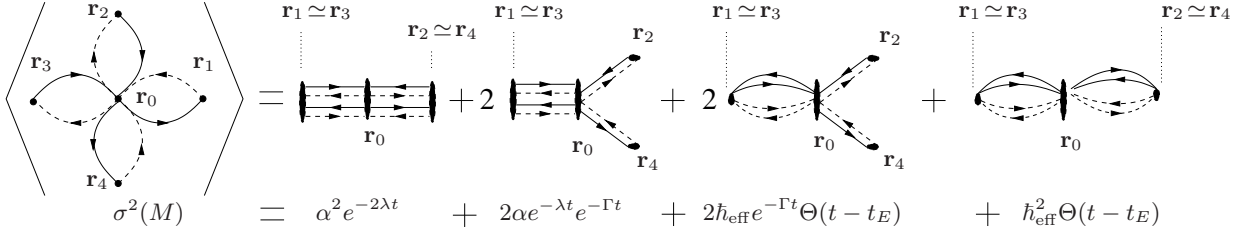


Figure 2: Diagrammatic representation of the averaged fidelity variance $\sigma^2(M)$ and the three time-dependent contributions that dominate semiclassically, together with the contribution giving the long-time saturation of $\sigma^2(M)$.

of $\delta\Phi_s$ as we will see momentarily). For long enough times, $t \gg t^*$, the phases $\delta\Phi_s$ fluctuate randomly and exhibit no correlation between different trajectories [20]. One thus applies the Central Limit Theorem (CLT) $\langle \exp[i\delta\Phi_s] \rangle = \exp[-\langle \delta\Phi_s^2 \rangle / 2] \simeq \exp[-\epsilon^2 \int dt \langle \nabla V(0) \cdot \nabla V(t) | \mathbf{r}_1 - \mathbf{r}_3 |^2 / 2\lambda]$. After performing a change of integration variable $\int d\mathbf{r} \sum_s C_s = \int d\mathbf{p}$ and using the asymptotic expression $C_s \simeq (m/t)^d \exp[-\lambda t]$ [21], one gets

$$\sigma_1^2 = \alpha^2 \exp[-2\lambda t], \quad (8a)$$

$$\alpha = \left(\frac{\lambda \nu^2 m^2}{\epsilon^2 t^2 \int d\tau \langle \nabla V(0) \cdot \nabla V(\tau) \rangle} \right)^{d/2}. \quad (8b)$$

The second dominant term is obtained from $s_1 = s_2 \simeq s_7 = s_8$, $s_3 = s_4$ and $s_5 = s_6$, with $\mathbf{r}_1 \simeq \mathbf{r}_3$, or equivalently $s_1 = s_2$, $s_7 = s_8$ and $s_3 = s_4 \simeq s_5 = s_6$ with $\mathbf{r}_2 \simeq \mathbf{r}_4$. Therefore this term comes with a multiplicity of two, and one obtains

$$\begin{aligned} \sigma_2^2 &= 2 \left(\frac{\nu^2}{\pi} \right)^{2d} \left\langle \int d\mathbf{r}_1 d\mathbf{r}_3 \sum C_{s_1}^2 \right. \\ &\quad \times \exp[-2\nu^2 \delta \mathbf{p}_{s_1}^2 + i\delta\Phi_{s_1}] \Theta(\nu - |\mathbf{r}_1 - \mathbf{r}_3|) \left. \right\rangle \\ &\quad \times \left\langle \int d\mathbf{r}_2 \sum C_{s_3} \exp[-\nu^2 \delta \mathbf{p}_{s_3}^2 + i\delta S_{s_3}] \right\rangle^2, \quad (9) \end{aligned}$$

again with the restriction $|\mathbf{r}_1 - \mathbf{r}_3| \leq \nu$. To calculate the first bracket on the right-hand side of Eq. (9), we first average the complex exponential, assuming again that enough time has elapsed so that actions are randomized. The CLT gives $\langle \exp[i\delta S_{s_3}] \rangle = \exp(-\frac{1}{2} \langle \delta S_{s_3}^2 \rangle)$ with

$$\langle \delta S_{s_3}^2 \rangle = \epsilon^2 \int_0^t dt \int_0^t dt' \langle V[\mathbf{q}(t)] V[\mathbf{q}(t')] \rangle. \quad (10)$$

Here $\mathbf{q}(\tilde{t})$ lies on s_3 with $\mathbf{q}(0) = \mathbf{r}_0$ and $\mathbf{q}(t) = \mathbf{r}_2$. In hyperbolic systems, correlators typically decay exponentially fast,

$$\langle V[\mathbf{q}(\tilde{t})] V[\mathbf{q}(\tilde{t}')] \rangle \propto \exp[-\eta |t - t'|], \quad (11)$$

with an upper bound on η set by the smallest positive Lyapunov exponent [24]. One thus obtains $\langle \delta S_{s_3}^2 \rangle = \Gamma t$. Usually $\Gamma \propto \epsilon^2$ is identified with the golden rule spreading of eigenstates of H over those of H_0 [5, 7]. It is dominated by the short-time behavior of $\langle V[\mathbf{q}(\tilde{t})] V[\mathbf{q}(0)] \rangle$.

We stress however that for long enough times, $\langle \delta S_{s_3}^2 \rangle \propto t$ still holds to leading order even with a power-law decay of the correlator $\langle V[\mathbf{q}(\tilde{t})] V[\mathbf{q}(\tilde{t}')] \rangle \propto |t - t'|^{-\eta}$, provided η is sufficiently large, $\eta \geq 1$. We note that similar expressions as Eq. (10) relating the decay of \overline{M} to time integrations over the perturbation correlator have been derived in Refs. [6, 19] using a different approach than the semiclassical method of Ref. [4] used here. Further using the sum rule

$$(\nu^2/\pi)^d \left(\int d\mathbf{r} \sum C_s \exp[-\nu^2 \delta \mathbf{p}_s^2] \right)^2 = 1, \quad (12)$$

one finally obtains

$$\sigma_2^2 = 2\alpha \exp[-\lambda t] \exp[-\Gamma t]. \quad (13)$$

The third and last dominant time-dependent term arises from either $s_1 = s_7$, $s_2 = s_8$, $s_3 = s_4$, $s_5 = s_6$ and $\mathbf{r}_1 \simeq \mathbf{r}_3$, or $s_1 = s_2$, $s_3 = s_5$, $s_4 = s_6$, $s_7 = s_8$ and $\mathbf{r}_2 \simeq \mathbf{r}_4$. It thus also has a multiplicity of two and reads

$$\begin{aligned} \sigma_3^2 &= 2 \left(\frac{\nu^2}{\pi} \right)^{2d} \left\langle \int d\mathbf{r}_1 d\mathbf{r}_2 d\mathbf{r}_3 d\mathbf{r}_4 \sum C_{s_1} C_{s_2} C_{s_3} C_{s_5} \right. \\ &\quad \times \exp[-\nu^2 (\delta \mathbf{p}_{s_1}^2 + \delta \mathbf{p}_{s_2}^2 + \delta \mathbf{p}_{s_3}^2 + \delta \mathbf{p}_{s_5}^2)] \\ &\quad \times \exp[i(\delta S_{s_3} - \delta S_{s_5})] \Theta(\nu - |\mathbf{r}_1 - \mathbf{r}_3|) \left. \right\rangle. \quad (14) \end{aligned}$$

The integrations, again, have to be performed with $|\mathbf{r}_1 - \mathbf{r}_3| \leq \nu$. We incorporate this restriction in the calculation by making the ergodicity assumption, setting

$$\begin{aligned} &\left\langle \int d\mathbf{r}_1 d\mathbf{r}_2 d\mathbf{r}_3 d\mathbf{r}_4 \dots \Theta(\nu - |\mathbf{r}_1 - \mathbf{r}_3|) \right\rangle \\ &= \hbar_{\text{eff}} \left\langle \int d\mathbf{r}_1 d\mathbf{r}_2 d\mathbf{r}_3 d\mathbf{r}_4 \dots \Theta(t - t_E) \right\rangle, \quad (15) \end{aligned}$$

which is valid for times larger than the Ehrenfest time [25] (for shorter times, $t < t_E$, the third diagram on the right-hand side of Fig. 2 goes into the second one). One then averages the phases using the CLT to get

$$\sigma_3^2 = 2\hbar_{\text{eff}} \exp[-\Gamma t] \Theta(t - t_E). \quad (16)$$

Subdominant terms are obtained by higher-order contractions (e.g. setting $\mathbf{r}_2 \simeq \mathbf{r}_4$ in the second and third graphs on the right hand-side of Fig.2). They either decay faster, or are of higher order in \hbar_{eff} , or both. We only

discuss the term which gives the long-time saturation at the ergodic value $\sigma^2(M) \simeq \hbar_{\text{eff}}^2$. For $t > t_E$, there is a phase-free (and hence time-independent) contribution with four different paths, resulting from the contraction $s_1 = s_7, s_2 = s_8, s_3 = s_5, s_4 = s_6$, and $\mathbf{r}_1 \simeq \mathbf{r}_3, \mathbf{r}_2 \simeq \mathbf{r}_4$. Its contribution is sketched as the fourth diagram on the right-hand side of Fig. 2. It gives

$$\sigma_4^2 = \left(\frac{\nu^2}{\pi}\right)^{2d} \left\langle \int d\mathbf{r}_1 d\mathbf{r}_3 \sum C_{s_1} C_{s_2} \times \exp[-\nu^2(\delta\mathbf{p}_{s_1}^2 + \delta\mathbf{p}_{s_2}^2)] \Theta(\nu - |\mathbf{r}_1 - \mathbf{r}_3|) \right\rangle^2. \quad (17)$$

From the sum rule of Eq. (12), and again invoking the long-time ergodicity of the semiclassical dynamics, Eq. (15), one obtains the long-time saturation of $\sigma^2(M)$,

$$\sigma_4^2 = \hbar_{\text{eff}}^2 \Theta(t - t_E). \quad (18)$$

Note that for $t < t_E$, this contribution does not exist by itself and is included in σ_1^2 , Eq. (8).

According to our semiclassical approach, the fidelity has a variance given to leading order by the sum of the four terms of Eqs. (8), (13), (16) and (18)

$$\sigma_{\text{sc}}^2 = \alpha^2 \exp[-2\lambda t] + 2\alpha \exp[-(\lambda + \Gamma)t] + 2\hbar_{\text{eff}} \exp[-\Gamma t] \Theta(t - t_E) + \hbar_{\text{eff}}^2 \Theta(t - t_E). \quad (19)$$

Eq. (19) is the central result of this paper. We see that for short enough times, i.e. before ergodicity and the saturation of $M(t) \simeq \hbar_{\text{eff}}$ and $\sigma^2(M) \simeq \hbar_{\text{eff}}^2$ is reached, the first term on the right-hand side of (19) will dominate as long as $\lambda < \Gamma$. For $\lambda > \Gamma$ on the other hand, $\sigma^2(M)$ exhibits a behavior $\propto \exp[-(\lambda + \Gamma)t]$ for $t < t_E$, turning into $\propto \hbar_{\text{eff}} \exp[-\Gamma t]$ for $t > t_E$. Thus, contrary to \overline{M} , $\sigma^2(M)$ allows to extract the Lyapunov exponent from the second term on the right-hand side of Eq. (19) even when $\lambda > \Gamma$. Also one sees that, unlike the strong perturbation regime $\Gamma \gg B$ [18], $M(t)$ continues to fluctuate above the residual variance $\simeq \hbar_{\text{eff}}^2$ up to a time $\simeq \Gamma^{-1} |\ln \hbar_{\text{eff}}|$ in the semiclassical regime $B > \Gamma > \Delta$. For $\Gamma \ll \lambda$, $\Gamma^{-1} |\ln \hbar_{\text{eff}}| \gg t_E$ and $M(t)$ fluctuates beyond t_E .

The above semiclassical approach breaks down at short times for which not enough phase is accumulated to motivate a stationary phase approximation [27]. To get the short-time behavior of $\sigma^2(M)$, we instead Taylor expand the time-evolution exponentials $\exp[\pm iH_{(0)}t] = 1 \pm iH_{(0)}t - H_{(0)}^2 t^2/2 + \dots + O(H_{(0)}^5 t^5)$. The resulting expression for $\sigma^2(M)$ contains matrix elements such as $\langle \psi_0 | H_{(0)}^a | \psi_0 \rangle$, $a = 1, 2, 3, 4$, which one then calculates using a Random Matrix Theory (RMT) approach [26] for the chaotic quantized Hamiltonian $H_{(0)}$ [5, 8, 19]. Keeping non-vanishing terms of lowest order in t , one has a quartic onset $\sigma^2(M) \simeq (\overline{\Sigma^4} - \overline{\Sigma^2}^2)t^4$ for $t \ll \Sigma^{-1}$, with $\Sigma^a \equiv [\epsilon^2(\langle \psi_0 | V^2 | \psi_0 \rangle - \langle \psi_0 | V | \psi_0 \rangle^2)]^{a/2}$. RMT gives $(\overline{\Sigma^4} - \overline{\Sigma^2}^2) \propto (\Gamma B)^2$, with a system-dependent prefactor of order one. From this and Eq. (19) one concludes that

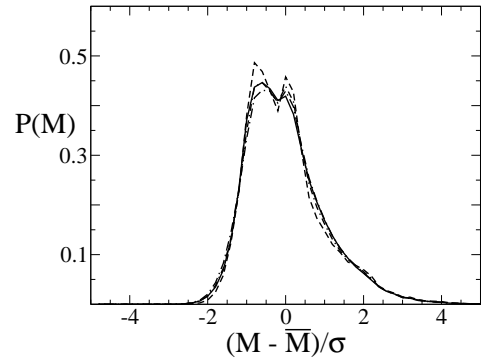


Figure 3: Distribution $P(M)$ of the fidelity computed for 10^4 different ψ_0 for $N = 32768$, $\delta K = 5.75 \cdot 10^{-5}$ (i.e. $\Gamma \approx 0.09$), at times $t = 25, 50, 75$ and 100 kicks.

$\sigma^2(M)$ has a nonmonotonous behavior, i.e. it first rises at short times, until it decays after a time t_c which one can evaluate by solving $\sigma_{\text{sc}}^2(t_c) = (\Gamma B)^2 t_c^4$. In the regime $B > \Gamma > \lambda$ one gets

$$t_c = \left(\frac{\alpha_0}{\Gamma B}\right)^{1/2+d} \left[1 - \lambda \left(\frac{\alpha_0}{\Gamma B}\right)^{1/2+d} \frac{1}{2+d} + O\left(\lambda^2 \left\{\frac{\alpha_0}{\Gamma B}\right\}^{2/2+d}\right) \right], \quad (20)$$

and thus

$$\sigma^2(t_c) \simeq (\Gamma B)^2 \left(\frac{\alpha_0}{\Gamma B}\right)^{4/2+d} \left[1 - \frac{4\lambda}{2+d} \left(\frac{\alpha_0}{\Gamma B}\right)^{1/2+d} + O\left(\lambda^2 \left\{\frac{\alpha_0}{\Gamma B}\right\}^{2/2+d}\right) \right]. \quad (21)$$

We explicitly took the t -dependence $\alpha(t) = \alpha_0 t^{-d}$ into account. We estimate that $\alpha_0 \propto (\Gamma \lambda)^{-d/2}$ (obtained by setting the Lyapunov time equal to few times the time of flight through a correlation length of the perturbation potential, as is the case for billiards or maps), to get $\sigma^2(t_c) \propto (B/\lambda)^{2d/2+d} \gg 1$. Because $0 \leq M(t) \leq 1$, this value is however bounded by $\overline{M}^2(t_c)$. Since in the other regime $\Gamma \ll \lambda$, one has $\sigma^2(t_c) \simeq 2\hbar_{\text{eff}} [1 - (2\hbar_{\text{eff}})^{1/4} \sqrt{\Gamma/B}]$ we predict that $\sigma^2(t_c)$ grows during the crossover from $\Gamma \ll \lambda$ to $\Gamma > \lambda$, until it saturates at a non-self-averaging value, $\sigma(t_c)/\overline{M}(t_c) \approx 1$, independently on \hbar_{eff} and B , with possibly a weak dependence on Γ and λ .

We conclude this analytical section by mentioning that applying the RMT approach to longer times reproduces Eq. (19) with $\lambda \rightarrow \infty$ [28]. This reflects the fact that RMT is strictly recovered for $t_E = 0$ only.

To illustrate our results, we present some numerical data. We based our simulations on the kicked rotator model with Hamiltonian [29]

$$H_0 = \frac{\hat{p}^2}{2} + K_0 \cos \hat{x} \sum_n \delta(t - n). \quad (22)$$

We concentrate on the regime $K > 7$, for which the dynamics is fully chaotic with a Lyapunov exponent $\lambda = \ln[K/2]$. We quantize this Hamiltonian on a torus, which requires to consider discrete values $p_l = 2\pi l/N$ and $x_l = 2\pi l/N$, $l = 1, \dots, N$, hence $\hbar_{\text{eff}} = 1/N$. The fidelity (1) is computed for discrete times $t = n$, as

$$M(n) = |\langle \psi_0 | (U_{\delta K}^*)^n (U_0)^n | \psi_0 \rangle|^2 \quad (23)$$

using the unitary Floquet operators $U_0 = \exp[-i\hat{p}^2/2\hbar_{\text{eff}}] \exp[-iK_0 \cos \hat{x}/\hbar_{\text{eff}}]$ and $U_{\delta K}$ having a perturbed Hamiltonian H with $K = K_0 + \delta K$. The quantization procedure results in a matrix form of the Floquet operators, whose matrix elements in x -representation are given by

$$(U_0)_{l,l'} = \frac{1}{\sqrt{N}} \exp[i\frac{\pi(l-l')^2}{N}] \exp[-i\frac{NK_0}{2\pi} \cos \frac{2\pi l'}{N}].$$

The local spectral density of eigenstates of $U_{\delta K}$ over those of U_0 has a Lorentzian shape with a width $\Gamma \propto (\delta K/\hbar_{\text{eff}})^2$ (there is a weak dependence of Γ in K_0) in the range $B = 2\pi \gtrsim \Gamma > \Delta = 2\pi/N$. This is illustrated in the inset to Fig. 6.

Numerically, the time-evolution of ψ_0 in the fidelity, Eq. (23), is calculated by recursive calls to a fast-Fourier transform routine. Thanks to this algorithm, the matrix-vector multiplication $U_{0,\delta K}\psi_0$ requires $O(N \ln N)$ operations instead of $O(N^2)$, and thus allows to deal with very large system sizes. Our data to be presented below correspond to system sizes of up to $N \leq 262144 = 2^{18}$ which still allowed to collect enough statistics for the calculation of $\sigma^2(M)$.

We now present our numerical results. Fig. 3 shows the distribution $P(M)$ of $M(t)$ in the regime $\Gamma < \lambda$ for different times. It is seen that even though $P(M)$ is not normally distributed, it is still well characterized by its variance. A calculation of $\sigma^2(M)$ is thus meaningful.

We next focus on σ^2 in the golden rule regime with $\Gamma \ll \lambda$. Data are shown in Fig. 4. One sees that $\sigma^2(M)$ first rises up to a time t_c , after which it decays. The maximal value $\sigma^2(t_c)$ in that regime increases with increasing perturbation, i.e. increasing Γ . Beyond t_c , the decay of σ^2 is very well captured by Eq. (16), once enough time has elapsed. This is due to the increase of $\sigma^2(t_c)$ above the self-averaging value $\propto \hbar_{\text{eff}}$ as Γ increases. Once the influence of the peak disappears, the decay of $\sigma^2(M)$ is very well captured by σ_3^2 given in Eq. (16), without any adjustable free parameter. Finally, at large times, $\sigma^2(M)$ saturates at the value given in Eq. (18).

As δK increases, so does Γ and $\sigma^2(M)$ decays faster and faster to its saturation value until $\Gamma \gtrsim \lambda$. Once Γ starts to exceed λ , the decay saturates at $\exp(-2\lambda t)$. This is shown in Fig. 5, which corroborates the Lyapunov decay of $\sigma^2(M)$ predicted by Eqs. (8). Note that in Fig. 5, the decay exponent differs from the Lyapunov exponent $\lambda = \ln[K/2]$ due to the fact that the fidelity averages $\langle C_s \rangle \propto \langle \exp[-\lambda t] \rangle \neq \exp[-(\lambda)t]$ over finite-time fluctuations of the Lyapunov exponent [18].

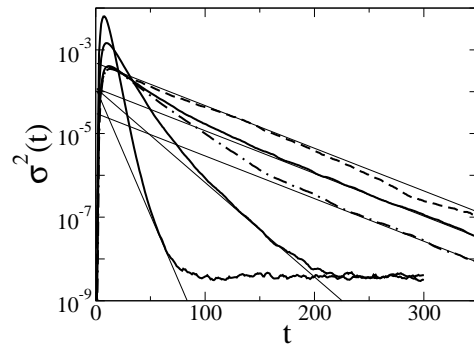


Figure 4: Variance $\sigma^2(M)$ of the fidelity vs. t for weak $\Gamma \ll \lambda$, $N = 16384$ and $10^5 \cdot \delta K = 5.9, 8.9$ and 14.7 (thick solid lines), $N = 4096$ and $\delta K = 2.4 \cdot 10^{-4}$ (dashed line) and $N = 65536$ and $\delta K = 1.48 \cdot 10^{-5}$ (dotted-dashed line). All data have $K_0 = 9.95$. The thin solid lines indicate the decays $= 2\hbar_{\text{eff}} \exp[-\Gamma t]$, with $\Gamma = 0.024(\delta K \cdot N)^2$ (there is no adjustable free parameter). The variance has been calculated from 10^3 different initial states ψ_0 .

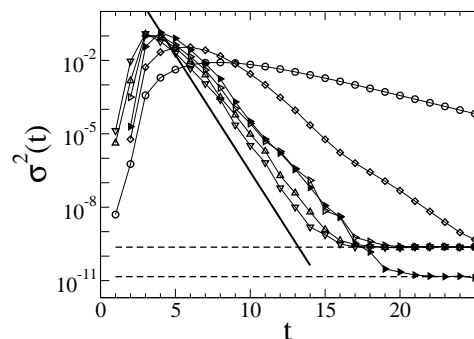


Figure 5: Variance $\sigma^2(M)$ of the fidelity vs. t in the golden rule regime with $\Gamma \gtrsim \lambda$ for $N = 65536$, $K_0 = 9.95$ and $\delta K \in [3.9 \cdot 10^{-5}, 1.1 \cdot 10^{-3}]$ (open symbols), and $N = 262144$, $K_0 = 9.95$, $\delta K = 5.9 \cdot 10^{-5}$ (full triangles). The solid line is $\propto \exp[-2\lambda_1 t]$, with an exponent $\lambda_1 = 1.1$, smaller than the Lyapunov exponent $\lambda = 1.6$, because the fidelity averages $\langle \exp[-\lambda t] \rangle$ (see text). The two dashed lines give $\hbar_{\text{eff}}^2 = N^{-2}$. In all cases, the variance has been calculated from 10^3 different initial states ψ_0 .

At long times, $\sigma^2(M)$ saturates at the ergodic value $\sigma^2(M, t \rightarrow \infty) = \hbar_{\text{eff}}^2$, as predicted. Finally, it is seen in both Figs. 4 and 5 that t_c decreases as the perturbation is cranked up. Moreover, there is no N -dependence of $\sigma^2(t_c)$ at fixed Γ . These two facts are at least in qualitative, if not quantitative, agreement with Eq. (20).

The behavior of $\sigma^2(t_c)$ as a function of Γ is finally shown in Fig. 6. First we show in the inset the behavior of the local spectral density

$$\rho(\epsilon) = \sum_{\alpha} |\langle \phi_{\beta}^{(0)} | \phi_{\alpha} \rangle|^2 \delta(\epsilon - \epsilon_{\alpha} + \epsilon_{\beta}), \quad (24)$$

of eigenstates $\{\phi_{\alpha}^{(0)}\}$ (with quasienergy eigenvalues ϵ_{α}) of U_0 over the eigenstates $\{\phi_{\alpha}\}$ (with quasienergy eigen-

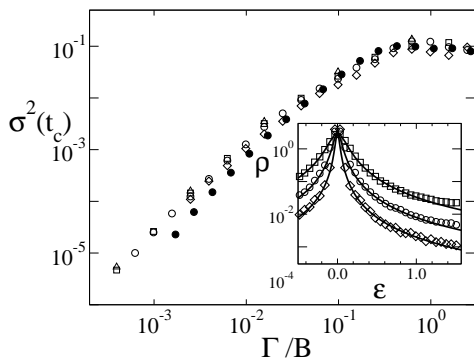


Figure 6: Maximal variance $\sigma^2(t_c)$ as a function of Γ/B , for $K_0 = 10.45$, $N = 4096, 16384, 65536$ and 262144 (empty symbols) and $K_0 = 50.45$, $N = 16384$ (full circles). The variance has been calculated from 10^3 different initial states ψ_0 . Inset: local spectral density of states $\rho(\epsilon)$ of eigenstates of an unperturbed kicked rotator with $K_0 = 12.56$ over the eigenstates of a perturbed kicked rotator with $K = K_0 + \delta K$, $\delta K = 5 \cdot 10^{-3}$. System sizes are $N = 250$ (diamonds), $N = 500$ (circles) and $N = 1000$ (squares). The solid lines are Lorentzian with widths $\Gamma \approx 0.0125, 0.05$ and 0.0124 in agreement with the formula $\Gamma = 0.024 (\delta K \cdot N)^2$.

values $\epsilon_\alpha^{(0)}$ of $U_{\delta K}$. As mentioned above, $\rho(\epsilon)$ has a Lorentzian shape with a width given by $\Gamma \approx 0.024(\delta K \cdot N)^2$. Having extracted the N - and δK -dependence of Γ , we next plot in the main part of Fig. 6 the maximum $\sigma^2(t_c)$ of the fidelity variance as a function of the rescaled width Γ/B of $\rho(\epsilon)$. As anticipated, $\sigma^2(t_c)$ first increases with Γ until it saturates at a value $\gtrsim 0.1$, independently on \hbar_{eff} , Γ or λ , once $\Gamma \approx B$. These data confirm Eq. (21) and the accompanying reasoning. Note that once Γ exceeds the bandwidth B , $\rho(\epsilon)$ is no longer Lorentzian, and the decay of both $M(t)$ and $\sigma^2(M)$ is no longer exponential [5].

In conclusion we have applied both a semiclassical and a RMT approach to calculate the variance $\sigma^2(M)$ of the fidelity $M(t)$ of Eq. (1). We found that $\sigma^2(M)$ exhibits a nonmonotonous behavior with time, first increasing algebraically, before decaying exponentially at larger times. The maximum value of $\sigma^2(M)$ is characterized by a non-self-averaging behavior when the perturbation becomes sizable against the system's Lyapunov exponent.

This work was supported by the Swiss National Science Foundation. We thank J.-P. Eckmann and P. Wittwer for discussions on structural stability, and Í. Adagideli for discussions at the early stage of this project.

-
- [1] F. Haake, *Quantum Signatures of Chaos* (Springer, Berlin, 2000).
- [2] R. Schack and C.M. Caves, Phys. Rev. Lett. **71**, 525 (1993).
- [3] A. Peres, Phys. Rev. A **30**, 1610 (1984).
- [4] R.A. Jalabert and H.M. Pastawski, Phys. Rev. Lett. **86**, 2490 (2001).
- [5] Ph. Jacquod, P.G. Silvestrov, and C.W.J. Beenakker, Phys. Rev. E **64**, 055203(R) (2001).
- [6] T. Prosen, T.H. Seligman, and M. Znidaric, Prog. Theor. Phys. Supp. **150**, 200 (2003).
- [7] N.R. Cerruti and S. Tomsovic, Phys. Rev. Lett. **88**, 054103 (2002).
- [8] F.M. Cucchiatti, C.H. Lewenkopf, E.R. Mucciolo, H.M. Pastawski, and R. O. Vallejos, Phys. Rev. E **65**, 046209 (2002).
- [9] D.A. Wisniacki and D. Cohen, Phys. Rev. E **66**, 046209 (2002).
- [10] Ph. Jacquod and D. L. Shepelyansky, Phys. Rev. Lett. **75**, 3501 (1995).
- [11] J. Vanicek and E.J. Heller, Phys. Rev. E **68**, 056208 (2003).
- [12] Y. Adamov, I.V. Gornyi, and A.D. Mirlin, Phys. Rev. E **67**, 056217 (2003).
- [13] Ph. Jacquod, Í. Adagideli, and C.W.J. Beenakker, Europhys. Lett. **61**, 729 (2003).
- [14] J. Emerson, Y.S. Weinstein, S. Lloyd, and D.G. Cory, Phys. Rev. Lett. **89**, 284102 (2002).
- [15] Ph. Jacquod, Í. Adagideli, and C.W.J. Beenakker, Phys. Rev. Lett. **89**, 154103 (2002).
- [16] A. Iomin, Phys. Rev. E **70**, 026206 (2004).
- [17] W. Wang, G. Casati, and B. Li, Phys. Rev. E **69**, 025201(R) (2004).
- [18] P.G. Silvestrov, J. Tworzydło, and C.W.J. Beenakker, Phys. Rev. E **67**, 025204(R) (2003).
- [19] T. Gorin, T. Prosen, and T.H. Seligman, New J. Phys. **6**, 20 (2004).
- [20] This time t^* is defined by $|\epsilon \int_0^{t^*} V(\mathbf{q}_s(t), t)| = 1$ for a typical trajectory s .
- [21] P. Cvitanović, R. Artuso, R. Mainieri, G. Tanner, and G. Vattay, *Chaos: Classical and Quantum*, ChaosBook.org (Niels Bohr Institute, Copenhagen 2003).
- [22] See e.g.: E.J. Heller and S. Tomsovic, Phys. Today **46**(7), 38 (1993).
- [23] Setting $s = s'$ for two trajectories generated by two different Hamiltonians $H = H_0 + \epsilon V$ is justified by the structural stability of hyperbolic systems for not too large ϵ ; see e.g.: A.B. Katok and B. Hasselblatt, *Introduction to the Modern Theory of Dynamical Systems* (Cambridge University Press, 1996). In the context of the fidelity, this point was first mentioned in Ref.[11].
- [24] P. Collet and J.-P. Eckmann, J. Stat. Phys. **115**, 217 (2004).
- [25] G.P. Berman and G.M. Zaslavsky, Physica A **91**, 450 (1978); M.V. Berry and N.L. Balasz, J. Phys. A **12**, 625 (1979).
- [26] M.L. Mehta, *Random Matrices* (Academic, New York, 1991).
- [27] This time is very short, of the order of the inverse energy of the particle, i.e. $O(\hbar_{\text{eff}}^2)$, where $a \geq 0$ depends on the system dimension and the energy-momentum relation. For $E \propto p^2$ and in two dimensions, one has $a = 1$.
- [28] C. Petitjean and Ph. Jacquod, unpublished (2004).
- [29] F. M. Izrailev, Phys. Rep. **196**, 299 (1990).